Copper Catalyzed Aryl Dehalogenation Reactions and their Inhibition

Th. Lippert, A. Wokaun

Physikalische Chemie II

D. Lenoir

Institut für Ökologische Chemie und Geochemie, Universität Bayreuth, D-8580 Bayreuth, Germany

Dioxin Mechanism of Formation / Inhibition / Spectroscopy, Infrared / Surfaces

The aryl coupling reaction of halobenzenes over alumina-supported copper catalysts has been studied by FTIR spectroscopy. Time-dependent changes in the spectra were recorded after stepwise addition of bromobenzene to the carrier gas stream. The coupling product, biphenyl, as produced by the copper-catalyzed "Ullmann type I" reaction, as well as phenol and phenolate species, have been observed. It was found that the thermal pretreatment of the supported catalyst has a pronounced influence on the rate of the catalytic bromobenzene conversion, and on the distribution of side products observed. Novel approaches to inhibit the catalytic dehydrogenation of aryl halides by ethanolamine addition to the catalyst have been studied for the investigated model reaction. The inhibitory action is due to both site blocking and irreversible deactivation of the copper surface due to nitride formation.

Introduction

Recent investigations on the mechanism of dioxine formation during combustion processes [1–3] have provided strong indications that these highly toxic compounds are formed from chlorinated phenol precursors. The presence of polychlorinated dibenzodioxines and dibenzo-furanes in municipal waste incineration (MWI) plants represents a serious problem [4] that has stimulated extensive research efforts in this field [5, 6]. It was suggested that fly ash particles act as catalysts in the synthesis of dibenzodioxines from monocyclic halogenated aromatic precursors [7, 8], which in turn are formed by "de novo" synthesis from a variety of organic and inorganic sources. In particular, the copper component of the fly ash particles was attributed a pivotal role in the catalytic mechanism [9].

In the present study, three aims have been pursued. First, supported copper catalysts are used to test whether some of the crucial steps involved in dioxine synthesis are indeed occurring on copper particle surfaces. In organic synthesis, the relevant transformations are known as "Ullmann type I" reaction [10–12] (bis-aryl formation from halobenzenes) and "Ullmann type II" reaction [13] (bis-aryl-ether formation from halogenated phenols) [14].

Second, it appeared of intrinsic interest to obtain more spectroscopic evidence on the mechanisms of the copper-catalyzed Ullmann reactions. There is no agreement in the literature as to whether Cu(0) [15, 16], Cu(I) [17, 18], or a mixture of both [19] are the catalytically active species. Several studies have shown the influence of a pretreatment of the copper (by ultrasound [20], electrolytic deposition [21], solvent cleaning, reduction of Cu(I) compounds [22], etc.). Furthermore, solvent [23] or atmosphere [24] have a profound influence on the catalytic activitiy. A variety of surface intermediates has been proposed, including radicals [25, 26], radical ions [27], ionic copper-aryl complexes [28–30], and covalent copper organic compounds [31–33].

Third, various techniques have been proposed [34] to remove the polychlorinated dioxines from the MWI exhaust gases, e.g. by filtering [35], pyrolysis of the dioxine molecules adsorbed on the fly ash particles [35], and dechlorination by the addition of water [36, 37]. Recently, attempts have been made [4] to inhibit the catalytic dioxine formation, by injecting ethanolamine or triethylamine into the post-combustion zone in a section where the gases have reached a temperature of 200 °C. In a pilot plant test [38], it was found that the dioxine concentration in the exhaust gas and on the fly ash particles was reduced by 95% when a triethanolamine/triethylamine mixture was injected continuously over an extended period of time. The inhibitory action developed only after an induction period of $\approx$8 hours.

If the model of copper-catalyzed synthesis correctly describes the mechanism of dioxine formation, then the inhibitory action of ethanolamine must be due to an interaction with the catalytic surface. In the final sections of this work, experiments aimed at elucidating this question will be reported.

Experimental

Apparatus

The setup used for the FTIR investigations consisted of a gas dosing system and an in situ IR transmission cell. The gas dosing facility was a slightly modified version of the design described by Jobson et al. [39]. For pulsewise addition, reactants were added to the carrier gas stream through an adapted gas chromatography injection port. Stepwise addition was realized by passing the carrier gas through a heated bubble column containing the reactant; the concentration was adjusted by varying the temperature of the bubble column, and hence the vapor pressure.

The IR cell reactor was designed similar to the one described in detail by Hecker and Bell [40]. The temperature in the reactor was controlled to within $\pm$3 K. The reactor was placed into the sample beam of the FTIR spectrometer (Mattson, model Polaris). Typically, 25 scans were coadded for each spectrum at a given temperature.

Catalyst and Reagents

The catalysts containing 10 wt.% of copper on alumina were prepared and reduced according to the procedure described in detail in Ref. [41]. Briefly, copper and aluminum hydroxides are coprecipitated in appropriate proportions, dried, calcined, and reduced in N_2/H_2 mixtures at 473 K. Depending on the calcination temperature, two different phases of the alumina support have been

Ber. Bunsenges. Phys. Chem. *94*, 1465–1471 (1990) –
0005–9021/90/1212–1465 $ 3.50+.25/0

obtained [42]. Mild calcination at 423 K resulted in a carrier containing abundant hydroxyl groups, AlO(OH), which was identified as the gibbsite modification by X-ray diffraction. The system containing 10 wt.% Cu on gibbsite will be denoted as "cat.A" in the following. By rigorous calcination at 873 K, the support was converted to γ-Al_2O_3; the corresponding catalyst is denoted as "cat.B".

Characteristic X-ray diffraction patterns are shown in Fig. 1. Globular copper particles are recognized in the scanning electron micrographs included in the figure. An average copper particle size of 19 nm was obtained from the observed X-ray line broadening [43], as analyzed by means of a deconvolution program, and was consistent with the particle size evaluated directly from the electron micrographs. The BET surface area was evaluated using nitrogen adsorption; values of 134 m^2/g and 175 m^2/g were found for catalysts A and B, respectively. Reference samples of unimpregnated support materials were obtained from Riedel-de-Haën (gibbsite) and from Merck ($\gamma-Al_2O_3$).

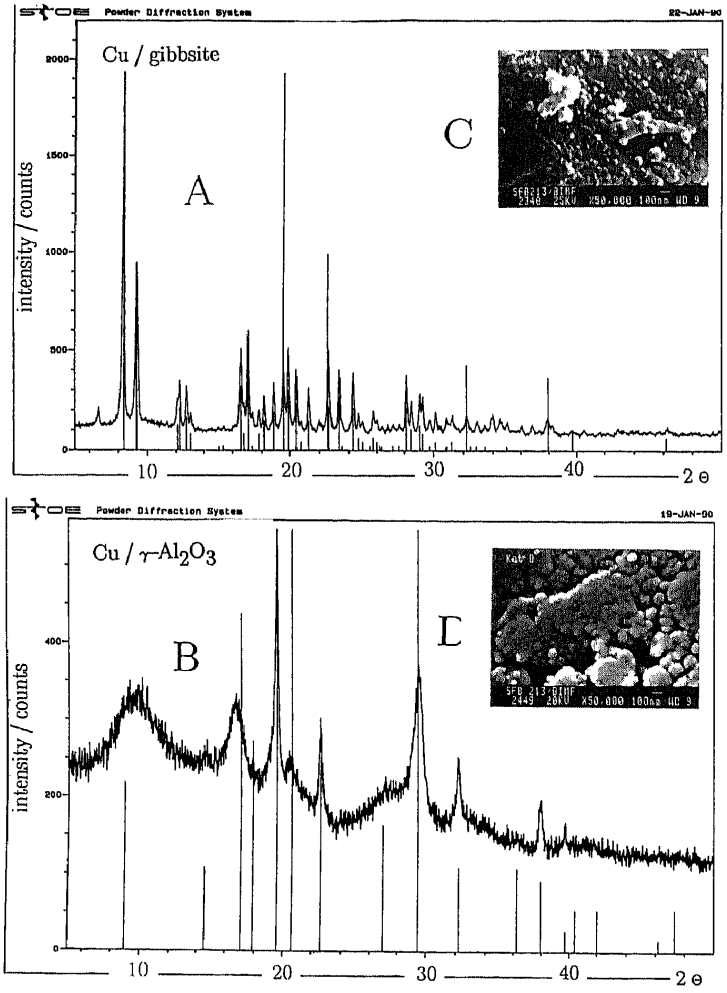

Fig. 1
X-ray spectra of alumina-supported copper catalysts. The support phases of catalysts "A" and "B" (see text) are identified as gibbsite (A) and γ-Al_2O_3 (B), respectively. Electron micrographs of an as-prepared catalyst, and of a wafer pressed at p = 12 tons cm^{-2} as used in the IR studies, are shown in (C) and (D)

For the IR studies, 40–60 mg of catalyst were pressed into thin wafers, of 20 mm diameter, using a pressure of 12 tons cm^{-2}. Electron micrographs taken on such a wafer (Fig. 1) show that the globular copper particles persist after pressing.

Bromobenzene (Aldrich, purity >99%) was purified from traces of water, by storing over molecular sieve. Ethanolamine (Aldrich, >98%) was used without further purification.

Catalyst Pretreatment and Measurement Procedure

Prior to the IR measurements, the wafers of catalyst or reference support material were pretreated in a flow (35 cm^3 min^{-1}) of pure nitrogen (Linde, 99.999%) at 473 K for two hours. In some experiments, the catalyst received a second reduction step in situ in the IR transmission cell. For this reduction, the catalyst was held at 473 K, while the hydrogen content in the nitrogen carrier gas stream was continuously increased from 0 to 100% over a period of 90 minutes. Subsequently, the catalyst was purged with pure nitrogen at 473 K or at 550 K for one hour.

After this sample pretreatment, a reference spectrum was collected: 25 scans were recorded at a resulution of 4 cm^{-1}. This spectrum served as the background for the following experiments. Subsequently, the reactants were added to the carrier gas, as detailed below. The flow of nitrogen was held constant at 35 cm^3 min^{-1} in all experiments.

Results

In this section, the following sets of experiments will be described. First, reference experiments on the unimpregnated alumina support materials are performed. Second, dehalogenation of bromobenzene is observed on catalysts of types A and B, with or without in situ reduction pretreatment of the catalyst. Third, inhibition of the dehalogenation reaction by addition of ethanolamine to the carrier gas stream is investigated.

When the pure gibbsite carrier (i.e., not containing copper) is held at 473 K and exposed to a stream of nitrogen containing 4 mole% of bromobenzene, the series of spectra shown in Fig. 2 is observed. The characteristic bands of bromobenzene at 1579, 1474, and 1445 cm^{-1} remain essentially unchanged. The only feature increasing with time is a broad band around 1260 cm^{-1} (see below).

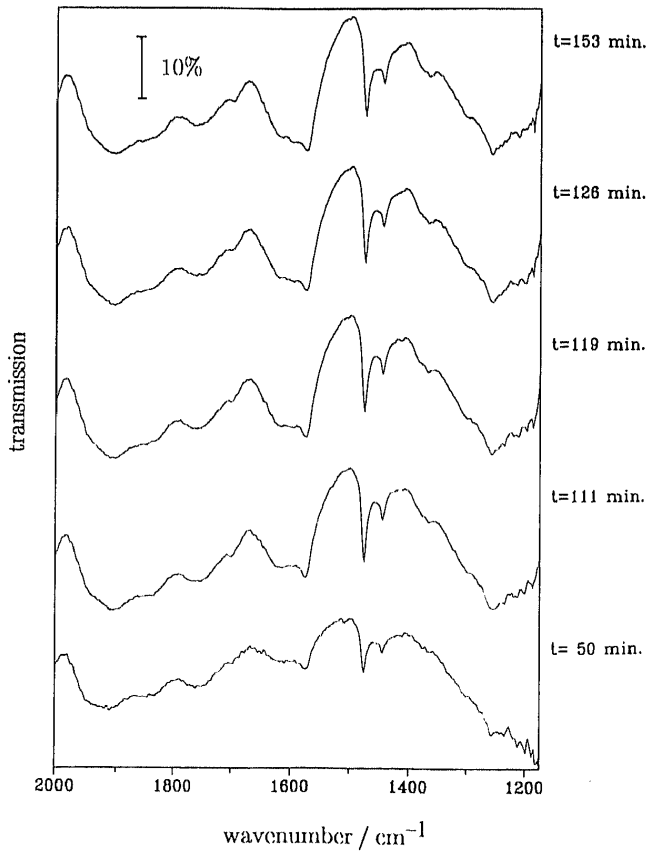

Fig. 2
Adsorption of bromobenzene on pure gibbsite at 473 K. Transmission spectra are monitored as function of time after the flow has been switched from pure nitrogen (35 cm^3/min) to 4 mole% of bromobenzene in nitrogen. 25 scans have been accumilated for each spectrum, at a resolution of 4 cm^{-1}

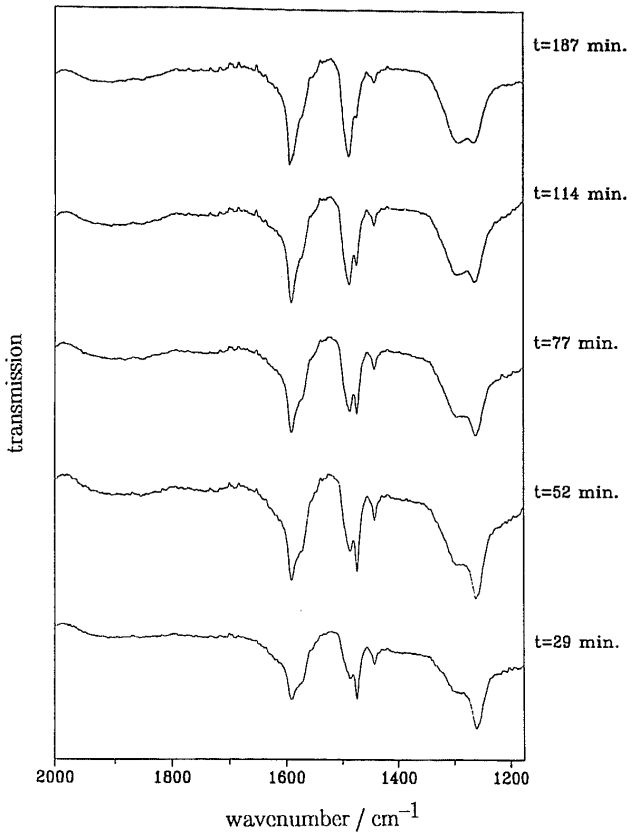

Fig. 3
Reactions of bromobenzene on a Cu/gibbsite catalyst (type A) held at 473 K, without in situ reduction. Experimental conditions are the same as in Fig. 2

Time dependent spectra observed on cat. A without in situ reduction pretreatment are shown in Fig. 3. Most prominent changes observed at 473 K are bands of increasing intensity at 1483 cm^{-1}, 1292–1285 cm^{-1}, and 1262–1259 cm^{-1}, whereas the parent compound absorptions are decreasing.

To assign the appearing bands, reference experiments have been performed in which the catalyst was loaded with possible products of the reaction. The coupling product, biphenyl, is characterized by bands at 1598, 1483, and 1432 cm^{-1}. This product is therefore responsible for the appearance of the intensive 1483 cm^{-1} absorption on the high frequency side of the disappearing 1474 cm^{-1} reactant band. In the C=C stretching region, the frequency difference between the absorptions of biphenyl (1598 cm^{-1}, medium) and bromobenzene (1579 cm^{-1}, strong), as determined for the reference compounds, is somewhat larger; however, the bands are broader and of unequal intensities. In Fig. 3, this frequency region too shows the increasing surface coverage of biphenyl, although reactant and product features are not resolved.

Table 1
Assignment of prominent bands observed

Frequency cm^{-1}	Molecule or species	Vibration
1579, 1474, 1445	bromobenzene	C–C stretching
1598, 1483, 1432	biphenyl	C–C stretching
1259	phenol	C–O stretching
1289	phenolate	C–O stretching
1610–1680	surface imine	C=N stretching
	surface aldehyde	C=O stretching
2130–2140	surface cyanide	C≡N stretching
	surface azide	N=N=N, asym. str.
2220–2250	surface azide	N=N=N, asym. str.

The two prominent appearing bands between 1300 and 1200 cm^{-1} are assigned to C–O stretching motions of phenol (1259 cm^{-1}) and of surface-bound phenolate ions (1289 cm^{-1}). The relevant assignments are summarized in Table 1.

Fig. 4 shows, for comparison, the same experiment performed on a sample of catalyst A that had been subjected to an in situ reduction treatment prior to bromobenzene adsorption. Adsorbate signals are considerably weaker, as compared to Fig. 3. Most noteworthy is the rapid formation of biphenyl: in the bottom trace recorded two minutes after the introduction of bromobenzene into the carrier gas stream, the biphenyl absorption at 1483 cm^{-1} has reached equal intensity as the parent bromobenzene absorption at 1474 cm^{-1}. The biphenyl surface coverage increases further as a function of time.

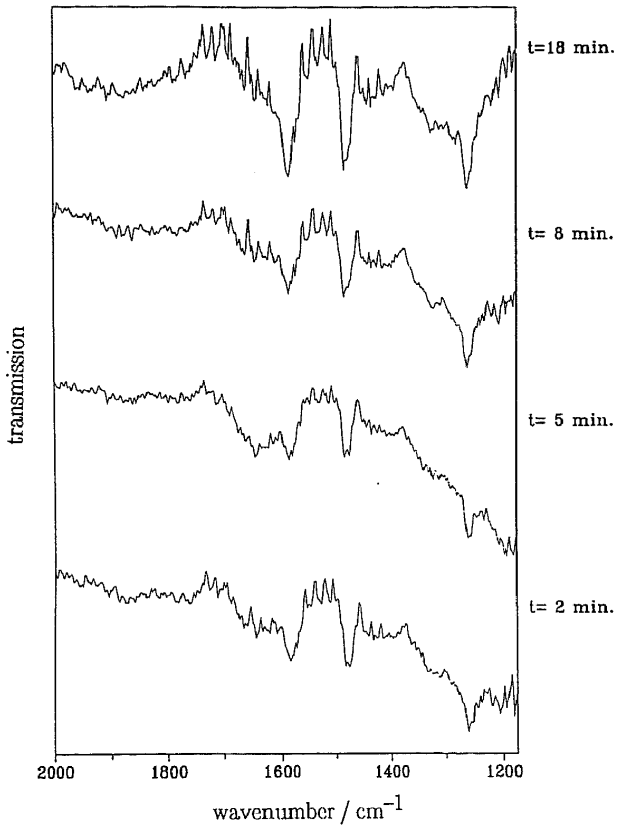

Fig. 4
Reactions of bromobenzene on a Cu/gibbsite catalyst (type A) held at 473 K, and pretreated by in situ reduction with hydrogen. Experimental conditions are the same as in Fig. 2

Corresponding experiments for catalysts of type B (γ-Al_2O_3-carrier) are documented in Figs. 5 and 6. The spectra exhibit the same sets of bands as observed with cat. A, but the rate of biphenyl formation is different. From a comparison of Figs. 3 and 5 (catalysts without in situ reduction) we recognize that copper on γ-Al_2O_3 is considerably more active than the corresponding catalyst on gibbsite support. The increase in bromobenzene conversion rate by in situ reduction of the copper, discussed above for type A catalysts, is also observed for copper on γ-Al_2O_3 (Fig. 6).

Finally, it appeared worthwhile to test the influence of the surface-bound water generated during the in situ reduction procedure. For this purpose, a type B catalyst was heated to 550 K in nitrogen for one hour, subsequent to in situ reduction. The corresponding spectra (Fig. 7) demonstrate that on this sample, the bromobenzene conversion rate is the fastest of all the samples discussed.

For a comparison of the various catalysts, we recall that we are monitoring changes in surface concentrations after switching on a continuous flow of bromobenzene in N_2. To obtain an estimate of turnover numbers, a quantity independent of the absolute surface

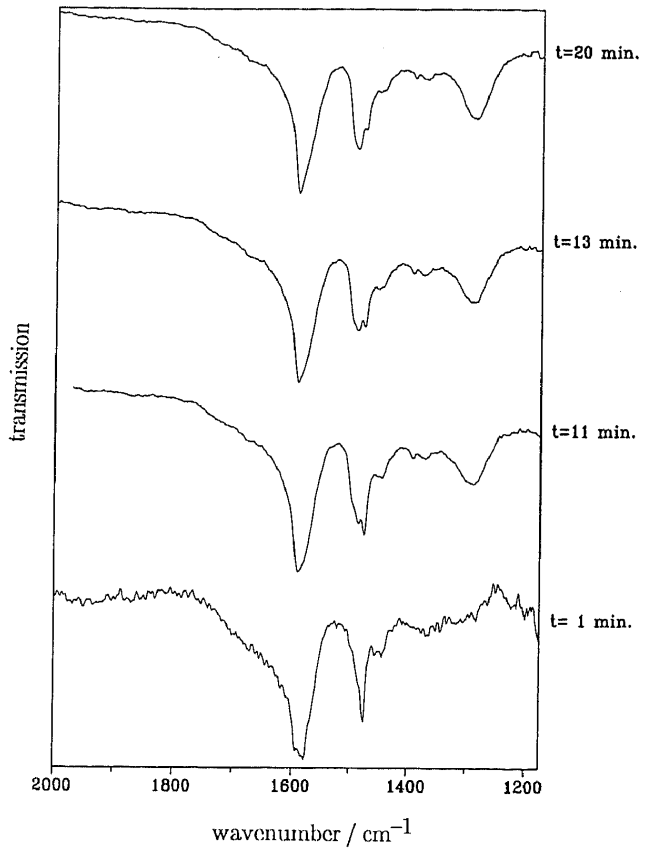

Fig. 5
Reactions of bromobenzene on a Cu/γ-Al_2O_3 catalyst (type B) held at 473 K, without in situ reduction. Experimental conditions are the same as in Fig. 2

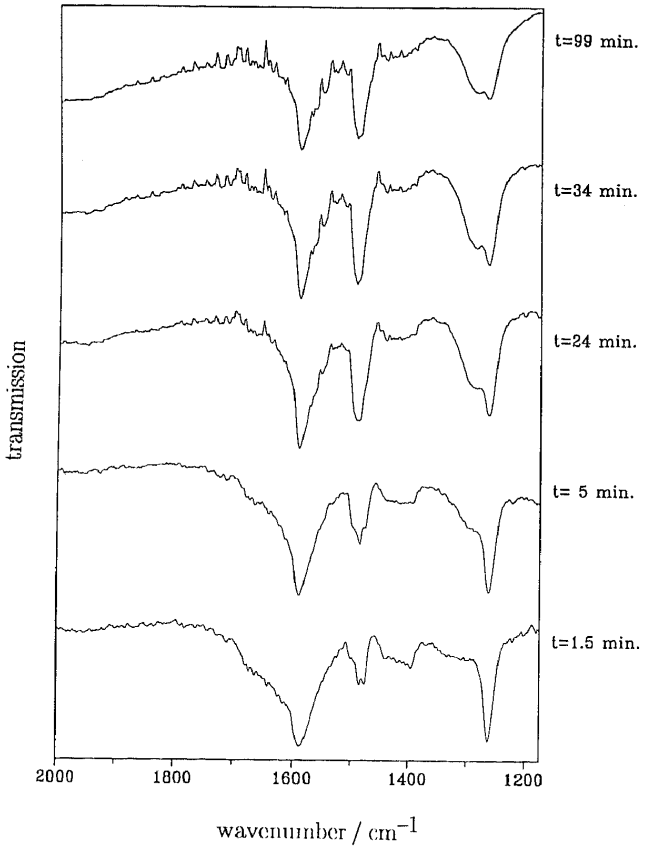

Fig. 6
Reactions of bromobenzene on a Cu/γ-Al_2O_3 catalyst (type B) held at 473 K, and pretreated by in situ reduction with hydrogen. Experimental conditions are the same as in Fig. 2

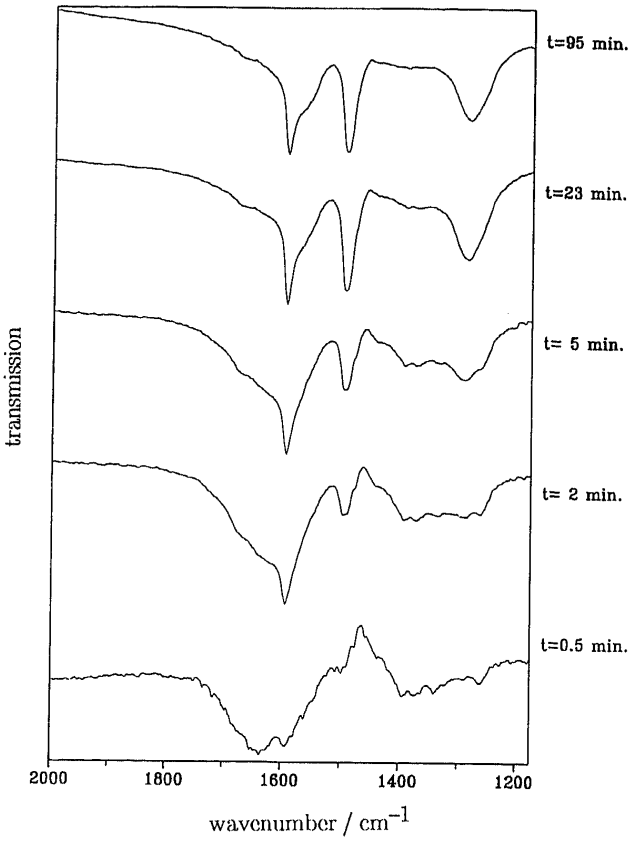

Fig. 7
Reactions at 473 K of bromobenzene on a Cu/γ-Al_2O_3 catalyst (type B) pretreated by in situ reduction with hydrogen at 473 K, followed by dehydration in nitrogen at 550 K. Experimental conditions are the same as in Fig. 2

coverage is desired. As a qualitative measure for the inverse surface reaction rate, we are using the time elapsed until the reactant (bromobenzene, 1474 cm^{-1}) and product (biphenyl, 1483 cm^{-1}) absorptions have reached equal intensities. These times are compiled in Table 2, for the catalysts characterized by the spectra in Figs. 3–7.

A nitrogen-cooled trap situated after the IR cell was used to condense the organic species leaving the catalytic reactor. After each catalytic run, the contents of the cold trap were analyzed by GC/MS. From the mass spectra, biphenyl was confirmed as the principal reaction product, besides large quantities of unreacted bromobenzene.

Subsequent to the reaction, the surface of a catalyst wafer was analyzed by energy dispersive X-ray analysis in the scanning electron microscope. A clear bromine signal was detected, showing that bromide released during the biphenyl formation (Ullmann type I reaction) was residing on the catalyst surface.

The inhibition of the debromination reaction was studied by injecting 5 μl of ethanolamine into the continuous N_2 carrier gas stream containing 4 mole% of bromobenzene. In the steady-state prior to injection, the catalyst surface is predominantly covered with the biphenyl coupling product. Time-dependent changes occurring subsequent to the ethanolamine injection are monitored in the spectra shown in Figs. 8 and 9. A broad band extending from 1610 to 1680 cm^{-1} appears, which will be discussed below. After ≈9 minutes the biphenyl band at 1483 cm^{-1} splits into two peaks. With increasing time, the biphenyl absorption continuously decreases in intensity, and the bromobenzene absorption at 1474 cm^{-1} reappears. Additional signals observed in the 2100–2300 cm^{-1} range (Fig. 9) will be assigned below.

When the contents of the cold trap were analyzed with GC/MS after the inhibition experiments, only the bromobenzene and ethanolamine reactant molecules were detected. By energy-dispersive X-ray analysis of the catalyst wafer after reaction a nitrogen peak was observed.

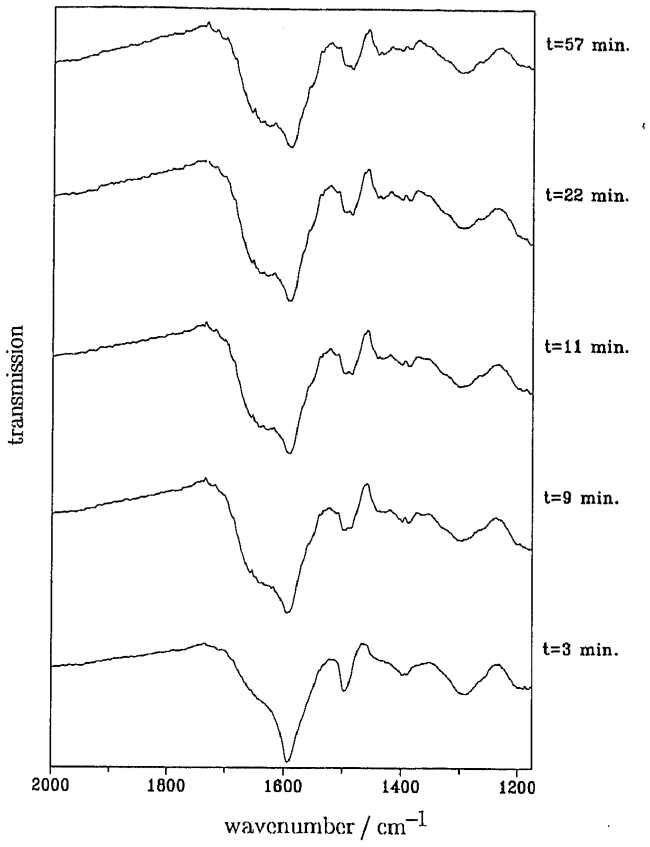

Fig. 8
Inhibition of the dehalogenation reaction by ethanolamine addition. A Cu/γ-Al_2O_2 catalyst held at 473 K is exposed to a continuous stream of 4 mole% bromobenzene in nitrogen (35 cm^3/min). Time-dependent changes in the 1200–2000 cm^{-1} region are monitored subsequent to injection of a pulse (5 µl) of ethanolamine at $t = 0$

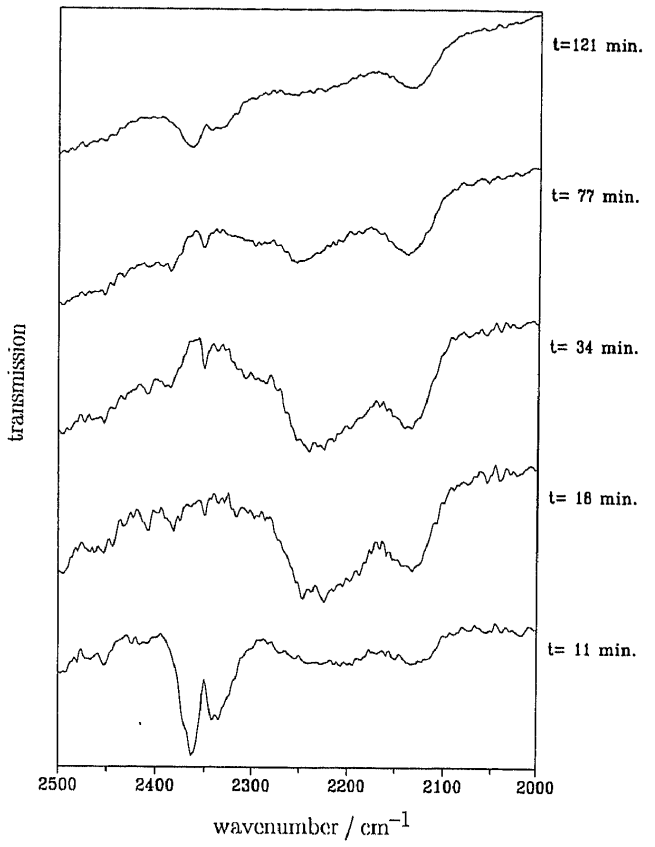

Fig. 9
Inhibition of the dehalogenation reaction by ethanolamine addition. A Cu/γ-Al_2O_3 catalyst held at 473 K is exposed to a continuous stream of 4 mole% bromobenzene in nitrogen (35 cm^3/min). Time-dependent changes in the 2000–2500 cm^{-1} region are monitored subsequent to injection of a pulse (5 µl) of ethanolamine at $t = 0$

Discussion

Observed Reactions and Influence of Catalyst Preconditioning

a) Phenol

The formation of phenol, as identified by the 1260 cm^{-1} absorption, was observed on pure gibbsite (Fig. 2), on gibbsite-supported catalysts (Figs. 3 and 4), as well as on γ-Al_2O_3-supported catalysts activated by in situ reduction. Common to these samples is an abundance of weakly bound surface hydroxyl groups, and/or surface bound water which results from the reduction of Cu_2O and CuO. Apparently, phenol is formed from bromobenzene by a substitution mechanism on the aromatic ring.

b) Phenolate

Surface phenolate is detected only on copper-containing catalysts; generally the signal at 1290 cm^{-1} increases with time on stream. In contrast, no phenolate signals are detected on the pure supports, even if, in addition, water is injected into the nitrogen carrier gas stream.

For the catalysts stored at ambient atmosphere prior to the experiment (Fig. 3 and 5), and not subject to in situ reduction, part of the surface copper is present in oxidized form (Cu_2O and/or CuO). It is then straightforward to formulate a substitution reaction in which the bromide substituent is replaced by surface O^{2-}, forming surface bound phenolate. This reaction is analogous to the formation of phenol from surface OH^-, discussed above.

On catalysts that are reduced in situ and then dehydrated at 550 K prior to bromobenzene addition, neither copper oxides nor surface water are available. Phenolate production on this catalyst (Fig. 7) likely involves the formation of copper-bound phenyl species, as discussed below, followed by the reaction of phenyl with O^{2-} ions of the support close to the copper/alumina grain boundaries. In this reaction, the surface phenyl species are transferred from the copper to the support, in a mechanism reminiscent of spill-over reactions [44, 45].

c) Biphenyl

Our observations regarding the rate of biphenyl formation are of interest in view of the different models for the mechanism of the copper-catalyzed Ullmann I reaction, mentioned in the introduction. The findings summarized in Table 2 clearly show that the catalysts subject to in situ reduction are more active than those stored at ambient conditions after preparation. This observation suggests that metallic copper, rather than one of the copper oxides, is the catalytically active species. Furthermore, the reaction rates are higher for copper supported on γ-Al_2O_3, as compared to the gibbsite support material, and they are highest on the catalyst that was dehydrated subsequent to in situ reduction. This demonstrates that surface hydroxyl groups are not in-

volved in the biphenyl formation. Taken together, these two results indicate that upon adsorption of bromobenzene to the copper particles of the catalyst, the phenyl-bromine bond is cleaved, and copper-bound phenyl species are formed. This mechanism is strongly supported by the observation of bromine in the EDX-spectra of the catalyst taken after reaction. Copper(I) bromide is likely to be formed on the catalyst surface.

Table 2
Relative dehalogenation activities of the catalysts observed[a)]

Pretreatment	Cu/gibbsite (cat. A)	Cu/γ-Al_2O_3 (cat. B)
no in situ reduction of catalyst	77 min (Fig. 3)	13 min (Fig. 5)
in situ reduction of catalyst	$\approx$2 min (Fig. 4)	$\approx$1 min (Fig. 6)
in situ reduction and dehydration of catalyst		<1 min (Fig. 7)

[a)] Table entries indicate time elapsed after bromobenzene addition to the catalyst when product (biphenyl, 1483 cm^{-1}) and reactant (bromobenzene, 1474 cm^{-1}) absorptions exhibit equal intensities.

The copper-phenyl species can recombine to form the biphenyl product (Langmuir-Hinshelwood mechanism). The alternative possibility that a surface phenyl group reacts with another bromobenzene molecule from the gas phase (Eley-Rideal mechanism) cannot be ruled out: Other authors have shown [46] that copper-phenyl and copper-halide molecules undergo rapid exchange reactions, such that the two mechanisms become indistinguishable.

Inhibition of Dehalogenation by Ethanolamine Addition

The results presented in Fig. 8 are in agreement with field tests in which the inhibition of dioxine formation by triethanolamine/triethylamine addition was studied [38]. Under the conditions of our experiment, the less volatile biphenyl is displaced from the surface over a period of $\approx$1 hour, and the catalyst is covered by unreacted bromobenzene. The additional bands appearing in Figs. 8 and 9 provide some indications on the mechanism of deactivation. The broad band between 1680 and 1610 cm^{-1} might be assigned to a surface-bound aldehyde [39], or else to a surface imine species [47, 48].

Both types of molecules have recently been identified as intermediates in the copper-catalyzed condensation reaction of aliphatic alcohols and amines on copper catalysts [49]. This class of reactions involves copper-catalyzed dehydrogenation and hydrogenation steps, and has been termed dehydroamination [50]. In our case, the ethanolamine inhibitor molecule contains both the amino and hydroxyl functional groups, and can undergo intermolecular dehydroamination reactions. Kinetic studies [49, 50] have shown that the dehydroamination reaction dominates on copper catalyst surfaces at the temperatures of our experiments, and displaces other feasible catalytic reactions such as amine disproportionation. As a consequence, one contribution to the inhibiting action of ethanolamine is based on competitive adsorption: bromobenzene is displaced from the catalytically active sites, which are blocked by the ethanolamine involved in dehydroamination reactions. [This picture is constistent with the observation that continuous triethanolamine/triethylamine addition is required in the field tests [38] to suppress the dioxine formation. However, the incineration reactor represents a much more complicated system, as catalytically active particles are continuously being reformed during the combustion process.]

Another contribution to the inhibitory action of ethanolamine is indicated by the bands observed in the 2100–2300 cm^{-1} range (Fig. 9). Only few functional groups absorbing in this frequency range are known. In a recent study of copper catalyst deactivation by ammonia in the absence of hydrogen, Kritzenberger et al. [51] have obtained evidence for the formation of surface azides characterized by band at 2130–2140 cm^{-1} and 2220–2250 cm^{-1}; upon prolonged exposure, the catalyst was deactivated by the formation of copper nitride on the surface [50, 52]. For substituted organic amine reactants, the formation of surface cyanides has been observed [48] on copper catalysts in the absence of hydrogen in the carrier gas; cyanides are again characterized by an absorption between 2100 and 2200 cm^{-1}. As our reactant, ethanolamine, can act both as a nitrogen and as a carbon source, the band observed at 2130 – 2140 cm^{-1} could be due to either azide or cyanide species. However, the frequency of the second feature observed in Fig. 9 (2220–2250 cm^{-1}) would be unusually high for cyanides, and therefore points to the presence of azides. In summary, the observation of two bands between 2100 and 2300 cm^{-1} points to incipient deactivation of the catalyst, as the mentioned species are potential intermediates in surface nitride formation [51]. Indeed, it has been shown [50, 52] that copper catalysts are inevitably deactivated under dehydroamination conditions if hydrogen is not present in the carrier gas stream.

Conclusion

The results of the present study show that Cu(0) is the catalytically active species in the copper-catalyzed bi-aryl synthesis from bromobenzene (Ullmann I reaction). Biphenyl is formed by the combination of copper-bound phenyl species. Fully reduced and dehydrated copper catalysts supported on γ-Al_2O_3 are most active among the catalyst systems characterized in this study.

As side products from the bromobenzene dehalogenation, phenol and surface-bound phenolate have been observed. Phenol is generated by a substitution reaction on support and catalyst surfaces which contain weakly bound hydroxyl groups. Surface phenolate is observed also on fully reduced and dehydrated Cu/γ-Al_2O_3 catalysts, and is likely to be produced by a spill-over of copper bound phenyl species, followed by reaction with O^{2-} groups of the support.

In the inhibition of the copper-catalyzed bromobenzene dehalogenation by ethanolamine, two mechanisms appear to be acting. First, the active sites of the catalyst are blocked by the adsorbed ethanolamine, which is involved in dehydroamination reactions that are favored on the catalyst. Second, the amine results in the irreversible deactivation of the catalyst by surface nitride formation, as evidenced by the

observation of azides and cyanides acting as intermediates in the deactivation process.

The authors would like to thank O. Hutzinger for his interest and support of this work. We are indebted to P. Barnickel and W. Häfner for help with the IR-experiments. Sincere thank are due to J. Klasmeier (GC/MS analyses), W. Reichstein (electron microscopy, EDX) and to Ch. Ross (X-ray diffraction experiments). Financial support by the Deutsche Forschungsgemeinschaft (SFB 213) is gratefully acknowledged.

References

[1] H. Vogg and L. Stieglitz (Eds.), Proceedings of the International Symposium on Chlorinated Dioxines and Related Compounds, Las Vegas 1987.
[2] F. W. Karasek and L. C. Dickson, Science *237*, 754 (1987).
[3] H. P. Hagenmaier, M. Kraft, H. Brunner, and R. Haag, Environ. Sci. Technol. *21*, 1080 (1987).
[4] L. C. Dickson, D. Lenoir, O. Hutzinger, K. P. Naikwadi, and F. W. Karasek, Chemosphere *16*, 777 (1987), and references therein.
[5] L. Stieglitz, Chemosphere *16*, 1917 (1987).
[6] L. C. Dickson and F. W. Karasek, J. Chromatogr. *389*, 127 (1987).
[7] T. J. Nestrick, L. L. Lamparski, and W. B. Crummet, Chemosphere *16*, 777 (1987).
[8] G. G. Choudry and O. Hutzinger, in: "Current Topics in Environmental and Toxicological Chemistry", Vol.IV, p. 170, eds. G. G. Choudry and O. Hutzinger, Gordon and Breach, New York 1983.
[9] L. C. Dickson, D. Lenoir, and O. Hutzinger, Proceedings of the 8th International Symposium on Chlorinated Dioxines and Related Compounds, Umea 1989.
[10] F. Ullmann, Annalen *332*, 28 (1904).
[11] P. E. Fanta, Synthesis *1*, 9 (1974).
[12] V. J. Koshelev, Ser. Khim. Nauk (4), *86* (1983).
[13] A. A. Moroz and M. S. Shvartsberg, Russ. Chem. Rev. *43*, 1443 (1974).
[14] H. Meerwein, in: "Methoden der Organischen Chemie" (Houben-Weyl), 4th ed., E. Müller (Ed.), Vol. VI/3, part 3, p. 86, Thieme, Stuttgart 1965; A. Streitwieser and C. H. Heathcock, "Organische Chemie", p. 1063, VCH, Weinhein 1986.
[15] M. S. Newmann and M. W. Logue, J. Org. Chem. *36*, 1398 (1978).
[16] J. C. Salfeld and E. Baume, Tetrahedron Lett. *28*, 3365 (1966).
[17] R. G. R. Bacon and S. G. Pande, J. Chem. Soc. (C), 1967 (1970).
[18] M. P. Cava and M. J. Mitchell, "Cyclobutadiene and Related Compounds", pp. 255 and 317, Academic Press, New York 1967.
[19] K. Fujimoto, S. Arita, and K. Takeshita, Yuki Gosei Kagaku Kyokai Shi *22*, 390 (1964); Chem. Abstr. *61*, 4245 (1964).
[20] J. Lindley, T. J. Mason, and J. P. Lorimer, Ultrasonics *25*, 45 (1987).
[21] Z, Kulicki and W. Karminski, Zesz. Nauk. Politech. Slask. Chem. *16*, 11 (1963).
[22] A. H. Lewin, M. J. Zovko, W. H. Rosewater, and T. Cohen, Chem. Commun., *80* (1987).
[23] W. Karminski and Z. Kulicki, Chem. Stosow. Ser. *A9*, 129 (1965); Chem. Abstr. *63*, 18018 (1965).
[24] R. B. Carlin and E. A. Swakon, J. Am. Chem. Soc. *77*, 966 (1955).
[25] H. W. E. Nursten, J. Chem. Soc., 3081 (1955).
[26] F. Bell and W. H. D. Morgan, J. Chem. Soc., 1716 (1954).
[27] V. V. Litvak and S. M. Schein, Zhur. Org. Khim. *11*, 903 (1975).
[28] P. E. Fanta, Chem. Rev. *64*, 613 (1964).
[29] Y. Mugnier and E. Laviron, J. Chem. Soc., Perkin Trans. II *9*, 1264 (1979).
[30] J. Forrest, J. Chem. Soc. 566, 574, 581, 589, 592, and 594, (1960).
[31] J. Lindley, Tetrahedron *40*, 1433 (1984).
[32] C. Bjorklund, Acta Chem. Scand. *25*, 2825 (1971).
[33] T. Cohen and T. Poeth, J. Am. Chem. Soc. *94*, 4363 (1972).
[34] for a recent survey, see e. g. M. J. Blümich, Nachr. Chem. Tech. Lab. *38*, 324 (1990).
[35] H. Vogg, J. Vehlow, and L. Stieglitz, VDI reports nos. 541 and 634 (1987).
[36] H. Vogg, M. Metzger, and L. Stieglitz, Waste Mgmt. Res. *5*, 285 (1987).
[37] H. Hagenmeier, Entsorgungspraxis *5*, 186 (1988); H. Brunner, R. Haag, and M. Kraft, VDI report no. 557 (1987).
[38] D. Lenoir, O. Hutzinger, E. Mützenich, and K. Horch, UWSF Z. Umweltchem. Ökotox. *1*, 3 (1989).
[39] E. Jobson, A. Baiker, and A. Wokaun, Ber. Bunsenges. Phys. Chem. *93*, 64 (1989).
[40] W. C. Hecker and A. T. Bell, J. Catal. *71*, 216 (1981).
[41] A. Baiker and W. Richarz, Synth. Commun. *8*, 27 (1978).
[42] E. Jobson, Ph. D. thesis, no. 8974, ETH Zürich 1989, p. 53.
[43] A. Baiker, Chimia *35*, 440 (1981); A. Baiker and M. A. Kohler, in "Handbook of Heat and Mass Transfer", Vol. *3*, N. P. Cheremisinoff (Ed.), Gulf 1989, p. 3.
[44] F. Solymosi, L. Volgyesi, and J. Sarkany, J. Catal. *54*, 336 (1978).
[45] F. Schüth and E. Wicke, Ber. Bunsenges. Phys. Chem. *92*, 813 (1988).
[46] M. Nilson and O. Wennerström, Acta Chem. Scand. *24*, 482 (1970).
[47] E. Jobson, A. Baiker, and A. Wokaun, J. Chem. Soc., Faraday Trans. *86*, 1131 (1990).
[48] R.Sokoll, H. Hobert, and J. Schmuck, J. Catal. *121*, 153 (1990).
[49] A. Baiker, W. Caprez, and W. L. Holstein, Ind. Eng. Chem. Prod. Res. Dev. *22*, 217 (1983).
[50] A. Baiker and J. Kijenski, Catal. Rev. Sci. Eng. *27*, 653 (1985).
[51] J. Kritzenberger, E. Jobson, A. Wokaun, and A. Baiker, Catal. Lett. *5*, 73 (1990).
[52] A. Baiker, D. Monti, and Y. Song Fan, J. Catal. *88*, 81 (1984).

(Eingegangen am 13. August 1990) E 7443

Ultrasonic Attenuation of an Isobutyric Acid/Water Mixture of Critical Composition

L. Belkoura, V. Calenbuhr, Th. Müller-Kirschbaum, and D. Woermann

Institut für Physikalische Chemie, Universität Köln, Luxemburger Straße 116, D-5000 Köln 41, West Germany

Critical Phenomena / Light, Scattering / Ultrasonic Absorption

Ultrasonic attenuation data (frequency range 10 MHz $< f <$ 45 MHz) of a binary isobutyric acid(COOH)/H_2O mixture and a pseudo-binary isobutyric acid(COOH)/H_2O, D_2O mixture of critical composition are analyzed in terms of the Ferrell-Bhattacharjee attenuation function $F(\Omega)$. The system specific parameter ω_0 necessary to calculate the temperature and frequency dependence of the universal reduced variable Ω is determined by static and dynamic light scattering experiments. It is found that $F(\Omega)$ fails to describe the ultrasonic attenuation